



Polymeric Micelle Assembly with Inorganic Nanosheets for Construction of Mesoporous Architectures with Crystallized Walls

Bishnu Prasad Bastakoti, Yunqi Li, Masataka Imura, Nobuyoshi Miyamoto, Teruyuki Nakato, Takayoshi Sasaki, and Yusuke Yamauchi*

Abstract: Here we propose a novel way to construct mesoporous architectures through evaporation-induced assembly of polymeric micelles with crystalline nanosheets. As a model study, we used niobate nanosheets exfoliated by the direct reaction of $K_4Nb_6O_{17} \cdot 3H_2O$ crystals with an aqueous solution of propylamine. The electrostatic interaction between negatively charged nanosheets and positively charged polymeric micelles enable us to form composite micelles with the nanosheets. Removal of the micelles by calcination results in robust mesoporous oxides with the original crystalline structure.

Co-assembly of soluble inorganic oligomers with amphiphilic molecules has been widely used to synthesize inorganic mesoporous materials.^[1] In most cases, the resultant frameworks are poorly crystallized or even amorphous, which limits their practical usage. Previously, mesoporous metal oxides with highly crystallized walls have been synthesized by using hard-templates (mesoporous silica or carbon).^[2] Although soft templates (such as block copolymers, ionic or nonionic surfactants) have been mostly used for preparation of mesoporous materials, careful post-treatment is required for improving the crystalline degree in the frameworks.^[3] However, we have often encountered several issues; incomplete crystallization, destruction of mesoporosity during crystallization, and crack formation because of stress associated during crystallization.

To overcome these issues, by using pre-formed nanocrystals as building units, several efforts have been made to

construct the crystalline frameworks. Several mesostructured inorganic/organic composites have been prepared through interaction between block copolymer templates and inorganic nanocrystals upon evaporation of solvent.^[4] After removal of the templates, the robust mesoporous structures can be obtained. Most of the previous reports have demonstrated the use of sub-10 nm nanocrystals and organic templates with neutral blocks. Although the mesoporous structures have been successfully obtained, the interaction between nanocrystals and polymer units is not clearly understood. Judicious selection of solvent compositions, careful understanding of the interactions of nanocrystals with block copolymers, and strict control on the evaporation rate for self-assembly are always critical factors.

In this communication we propose a more reliable way based on “colloidal chemistry” (Figure 1). Here, we focus on two-dimensional (2D) crystalline nanosheets^[5] as inorganic

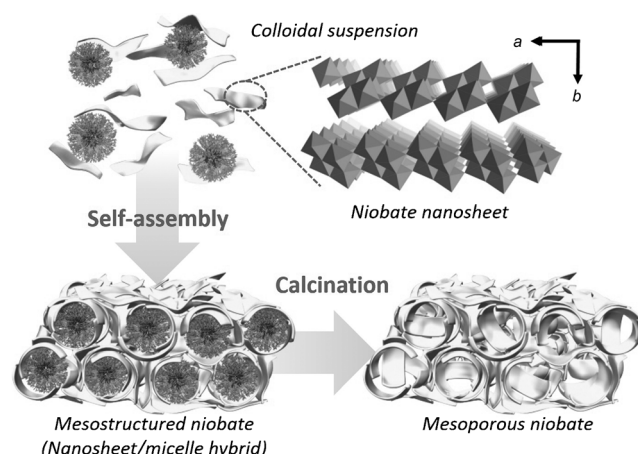


Figure 1. Synthesis of crystalline mesoporous materials from co-assembly of niobate nanosheets and polymeric micelles based on colloidal chemistry.

building blocks for the synthesis of mesoporous architectures, for the first time. The 2D nanosheets with thin thickness in atomic scale can be easily monodispersed under controlled conditions to show high colloidal stability in aqueous solution. Such charged nanosheets can interact with oppositely charged substances. This noticeable feature motivates us to use the charged nanosheets as building blocks for the synthesis of mesoporous materials.

Our synthetic protocol is shown in Figure 1. An aqueous micelle solution of an asymmetric triblock copolymer poly-

[*] Dr. B. P. Bastakoti, Y. Li, Prof. T. Sasaki, Prof. Y. Yamauchi

World Premier International Center for
Materials Nanoarchitectonics (WPI-MANA)
National Institute for Materials Science (NIMS)
1-1 Namiki, Tsukuba 305-0044 (Japan)
E-mail: Yamauchi.Yusuke@nims.go.jp
Homepage: <http://www.yamauchi-labo.com/>

Y. Li, Dr. M. Imura, Prof. Y. Yamauchi
Faculty of Science and Engineering, Waseda University
3-4-1 Okubo, Shinjuku, Tokyo 169-8555 (Japan)
Prof. N. Miyamoto
Department of Life, Environment and Materials Science
Faculty of Engineering, Fukuoka Institute of Technology
3-30-1, Wajiro-Higashi, Higashi, Fukuoka, Fukuoka 811-0295 (Japan)
Prof. T. Nakato
Department of Applied Chemistry
Kyushu Institute of Technology
1-1 Sensui-cho, Tobata, Kitakyushu, Fukuoka 804-8550 (Japan)



Supporting information for this article is available on the WWW
under <http://dx.doi.org/10.1002/anie.201410942>.

(styrene-*b*-2-vinylpyridine-*b*-styrene) (PS-PVP-PEO) was firstly prepared. The molecular weights of the PS, PVP, and PEO blocks were 13000, 9000, and 16500, respectively. In brief, 0.1 g of the polymer was dissolved in 4.5 g of *N,N*-dimethylformamide, in which the polymer was totally dissolved as unimers. To accelerate the micellization 0.5 g of distilled water was slowly added. The obtained solution was dialyzed against water to obtain the PS-PVP-PEO micelles. Finally, the polymer concentration was set to be 2 g L⁻¹. The pH of the solution was adjusted to 3 with a diluted HCl solution. Formation of very stable polymeric micelles with a hydrodynamic diameter of around 90 nm and a polydispersity index of 0.09 was confirmed by dynamic light scattering experiments (see Figure S1 in the Supporting Information). The Tyndall effect clearly confirmed the presence of stable colloidal particles (Figure 2b). Only the PS blocks of the

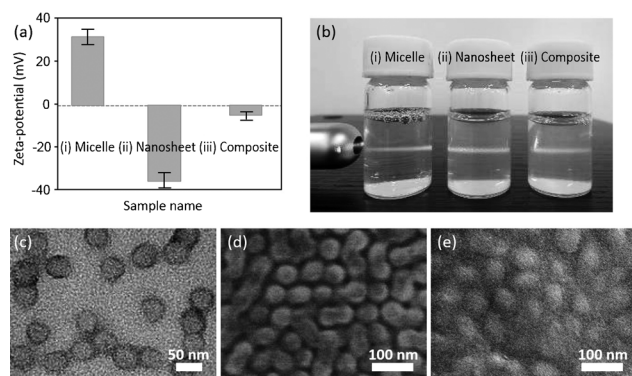


Figure 2. a) Zeta-potentials of i) polymeric micelles, ii) niobate nanosheets, and iii) composite micelles, b) photographs of the corresponding colloidal solutions, c) TEM images of polymeric micelles, and d, e) SEM images of polymeric micelles d) before and e) after addition of nanosheets.

polymeric micelles were stained with phosphotungstic acid (0.1 %) prior to TEM measurements.^[6] The TEM image shown in Figure 2c revealed that the micelle has a spherical structure. The PS core size was around 40 nm which is smaller than the hydrodynamic diameter of 90 nm with extended PVP and PEO chains. Because of the presence of the pH-sensitive PVP blocks, the surface charge of the micelles turned positive when the pH in the solution decreased to the pK_a (4.5) value of PVP.^[7] The zeta-potential measurement revealed that the micelles possess surface charges of +34 mV at pH 3 (Figure 2a). The positive zeta-potential is due to the protonation of PVP units, which allows the strong adherence of polymeric micelles towards any negatively charged substance.

As a model study, negatively charged niobate nanosheets were used as inorganic building blocks. $K_4Nb_6O_{17} \cdot 3H_2O$ crystals were delaminated into colloidal nanosheets by interaction with propylammonium (Figure 2bii). $K_4Nb_6O_{17} \cdot 3H_2O$ crystals are niobate-layered structures in which potassium ions are present in the interlayer space.^[8] Potassium (K^+) ions in the interlayer I are easily exchanged with propylammonium, while those in the interlayer II are relatively difficult to replace, thereby resulting in bilayer niobate nanosheets with a thickness of about 2 nm (Fig-

ure S2a). The colloidal solution containing the nanosheets (0.2 %) shows negative charge of -36 mV at pH 3 (Figure 2a). Therefore, the dispersed nanosheets can interact effectively with the positively charged micelles through electrostatic force.

Under typical conditions, 50 μ L of nanosheet colloidal solution (0.2 %) was mixed with 2 mL of polymeric micelles (2 g L⁻¹). The zeta-potential was again measured and found to be -3 mV (i.e., almost zero), indicating that the decoration of the nanosheets on the spherical polymeric micelles neutralizes the charges (Figure 2a). Even under almost zero-charge condition (+3 mV), the colloidal hybrid solution is very stable. This is because the PEO corona is still free which stabilizes the colloidal hybrid micelles by steric repulsion between the PEO chains. The same situation was also observed in a titanate nanosheet system^[9] prepared by interaction with $(C_4H_9)_4NOH$ (Figure S3). The colloidal suspension of nanosheet-decorated composite micelles was very stable without any precipitation (Figure 2biii and Figure S3biii). Even after one month, any precipitates were not confirmed at all (Figure S4).

The above-obtained suspension of nanosheet-decorated composite micelles was directly casted over either a silicon substrate or a glass substrate. Upon evaporation of the solvent, the composite micelles underwent their self-organization to form mesostructured niobate (i.e., a nanosheet/micelle hybrid film), as shown in Figure 1. The morphology of the dried sample was observed under scanning electron microscope (SEM). Spherical humps related to the presence of PS-PVP-PEO micelles were observed over the entire area and the micelle surface is completely covered with nanosheets (Figure 2e and Figure S5). In contrast, the polymeric micelles themselves self-assembled without nanosheets are clearer spherical objects (Figure 2d) with smooth surface.

In general, it has been known that the dispersed nanosheets interacting with propylammonium were restacked during the solvent evaporation to form the lamellar aggregates (Figure 3a). Sharp diffraction peaks can be indexed as $0k0$ ($k=2, 4, 6$), indicating the formation of a lamellar structure. However, when the nanosheets were assembled with the polymeric micelles, the peaks corresponding to interlayer spacing totally disappeared, although the 002 peak derived from the in-plane structure was preserved. We suggest that the strong electrostatic interaction of micelles

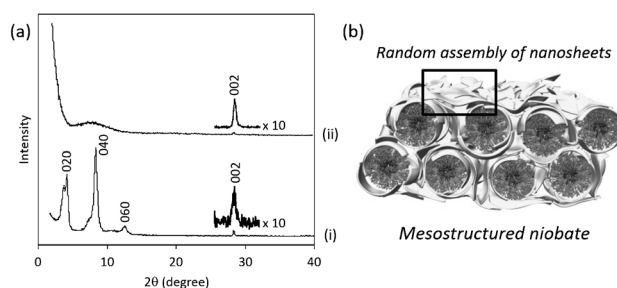


Figure 3. a) Wide-angle XRD patterns for i) nanosheet film prepared in the absence of polymeric micelles and ii) nanosheet/micelle hybrid film prepared in the presence of polymeric micelles. b) Random assembly of nanosheets on micelles.

with nanosheets disturbs the spontaneous assembly of the nanosheets; thereby losing well-stacked layered structure, as shown in Figure 3b. (The details are discussed in later section.) The same situation was observed in single titanate nanosheets (Figure S6).

To remove the polymer template, the samples were calcined at 500 °C. Calcination at 500 °C ensures the complete removal of polymer, as shown in Figure S7. From SEM images, mesopores were observed over the entire area (Figure S8). High-resolution SEM images show that the mesopore sizes were around 30–40 nm, which are almost the same as the PS core size in the used polymeric micelles (Figure 2c). As seen in Figure 4a and Figure S9, the nanosheets seem to be randomly assembled to form the pore walls. It should be noted that the mesopores are not in perfect spherical shape. A similar situation has been observed in nanocrystal-based mesoporous materials (Figure S10a), which is in contrast to general mesoporous metal oxides synthesized using small-sized inorganic oligomers or salts as precursors (Figure S10b). Actually, the average lateral size of the used nanosheets is around 200 nm (Figure S2a) which is a few times larger than the hydrodynamic diameter of the used micelles. Very thin nanosheets are flexible,^[10] so they can be curled and/or bended on the concave micelle surface. As shown in Figure S7, a large amount of gas (e.g., CO₂) evolved during the combustion of the polymer template breaks the thin nanosheets, which also induces the formation of open mesopores on the film surface.

From the high-resolution TEM images in Figure 4b and Figure S11, the presence of lattice fringes is clearly observed. The pores are indeed surrounded by crystalline nanosheets. As confirmed in Figure S12, it has been reported that niobate nanosheets interacting with propylammonium are stable up to 500 °C without recrystallization to other phases. It is interesting that selected-area electron diffraction (ED) patterns

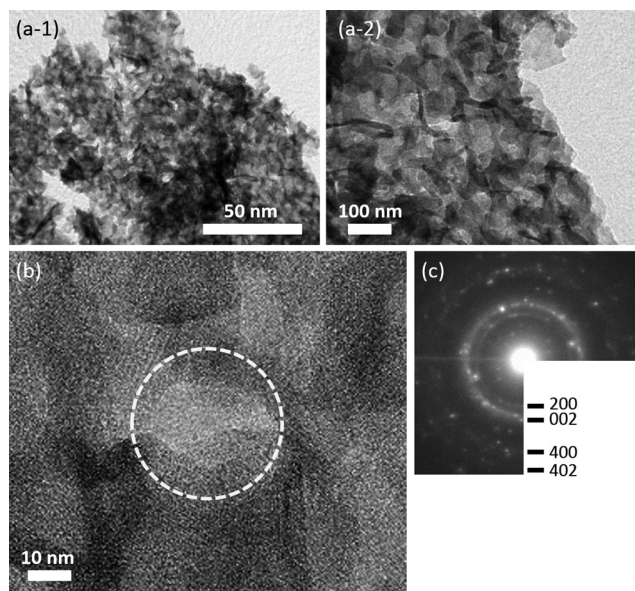


Figure 4. a) TEM image of mesoporous niobate after removal of the template. b) High-resolution TEM image of the crystalline framework. One mesopore is indicated by a dashed circle. c) Selected-area ED patterns taken from 10 000 nm² (100 nm × 100 nm).

taken from mesoporous niobate show mainly *h0l* diffractions derived from the original in-plane crystalline structure of the niobate nanosheets (Figure 4c). However, a single titanate nanosheet is thermally less stable, because its thickness^[9] (ca. 0.75 nm) is thinner than that of a niobate bilayer nanosheet (ca. 2.0 nm).^[8] Layered titanate nanosheets were destroyed above 350 °C by removing the intercalated organic amine and titanium dioxide started to be crystallized as anatase^[9] (Figure S13). Therefore, the anatase crystals were observed on the film surface after calcination at the same temperature (500 °C), as shown in Figure S14. In our system, the amount of added nanosheets is very important to obtain the final mesostructure (Figure S15). Under typical conditions, the zeta-potential is almost zero (Figure 2b), indicating the complete neutralization of negatively charged nanosheets by positively charged polymeric micelles, which is the ideal condition.

Here, we show the potential application of a mesoporous niobate film as an excellent photocatalyst for the degradation of methylene blue (MB) under UV irradiation (Figure S16). A large amount of MB dyes (14.02 w/w %) were adsorbed into/on a mesoporous niobate film. For comparison, K₄Nb₆O₁₇·3H₂O crystals before the exfoliation and niobate sample prepared without polymeric micelles were also tested. However, these adsorption amounts of MB dyes were quite small (5.28 w/w % and 6.98 w/w %, respectively). Considering the above results, the mesoporous niobate film shows superior MB adsorption capacity. More MB molecules can easily access and effectively adsorbed on the pore surface (i.e., nanosheet surface) through the open mesoporous architecture. After the adsorption, the solutions were irradiated with UV light. The mesoporous niobate film degraded 83.6 % of MB dyes within 70 minutes, which is much higher than the other two samples.

To conclude, we have proposed a novel synthetic way which makes possible effective interactions of colloidal niobate nanosheets with polymeric micelles. The advantages of our block copolymer over commercial block copolymers (F127 and P123 triblock copolymers) are:

- 1) Negatively charged colloidal particles (e.g. nanosheets) interact with positively charged templates. Nonionic micelles made of F127, P123 are not so effective.
- 2) Because of the presence of a very hydrophobic frozen polystyrene core with a hydrophilic PEO corona, the micelles are stably formed in solution.
- 3) The core size of the micelles is also critical for curling or bending of the nanosheets on the micelle surface. The curling or bending of the nanosheets is not easy when the core sizes are small (smaller than 10 nm in the cases of F127, P123).

Our smart synthesis is widely applicable to other inorganic nanosheets for preparation of mesoporous crystalline materials which could have an enormous potential and provide new functionality.

Keywords: block copolymers · mesoporous materials · micelle assembly · nanosheets · photocatalysis

How to cite: *Angew. Chem. Int. Ed.* **2015**, *54*, 4222–4225
Angew. Chem. **2015**, *127*, 4296–4299

- [1] a) Q. Lu, F. Gao, S. Komarneni, M. Chan, T. E. Mallouk, *J. Am. Chem. Soc.* **2004**, *126*, 8650–8651; b) C. Xiao, N. Fujita, K. Miyasaka, Y. Sakamoto, O. Terasaki, *Nature* **2012**, *487*, 349–353; c) W. Li, Z. Wu, J. Wang, A. A. Elzatahry, D. Zhao, *Chem. Mater.* **2014**, *26*, 287–298; d) Y. Yamauchi, *J. Ceram. Soc. Jpn.* **2013**, *121*, 831–840.
- [2] a) W. Yue, X. Xu, J. T. S. Irvine, P. S. Attidekou, C. Liu, H. He, D. Zhao, W. Zhou, *Chem. Mater.* **2009**, *21*, 2540–2546; b) H. Tüysüz, C. Weidenthaler, T. Grewe, E. L. Salabaş, M. J. B. Romero, F. Schüth, *Inorg. Chem.* **2012**, *51*, 11745–11752; c) H. Tüysüz, Y. Liu, C. Weidenthaler, F. Schüth, *J. Am. Chem. Soc.* **2008**, *130*, 14108–14110.
- [3] a) B. Lee, D. Lu, J. N. Kondo, K. Domen, *Chem. Commun.* **2001**, 2118–2119; b) B. Lee, T. Yamashita, J. N. Kondo, D. Lu, K. Domen, *Chem. Mater.* **2002**, *14*, 867–875; c) H. Miyata, M. Itoh, M. Watanabe, T. Noma, *Chem. Mater.* **2003**, *15*, 1334–1343; d) V. N. Urade, H. W. Hillhouse, *J. Phys. Chem. B* **2005**, *109*, 10538–10541.
- [4] a) T. Brezesinski, J. Wang, J. Polleux, B. Dunn, S. H. Tolbert, *J. Am. Chem. Soc.* **2009**, *131*, 1802–1809; b) T. Coquil, C. Reitz, T. Brezesinski, E. J. Nemanick, S. H. Tolbert, L. Pilon, *J. Phys. Chem. C* **2010**, *114*, 12451–12458; c) R. Buonsanti, T. E. Pick, N. Krins, T. J. Richardson, B. A. Helms, D. J. Milliron, *Nano Lett.* **2012**, *12*, 3872–3877; d) I. E. Rauda, R. Buonsanti, L. C. Saldarriaga-Lopez, K. Benjauthrit, L. T. Schelhas, M. Stefik, V. Augustyn, J. Ko, B. Dunn, U. Wiesner, D. J. Milliron, S. H. Tolbert, *ACS Nano* **2012**, *6*, 6386–6399; e) I. E. Rauda, V. Augustyn, B. Dunn, S. H. Tolbert, *Acc. Chem. Res.* **2013**, *46*, 1113–1124; f) D. J. Milliron, R. Buonsanti, A. Llordes, B. A. Helms, *Acc. Chem. Res.* **2014**, *47*, 236–246.
- [5] a) S. Ida, C. Ogata, M. Eguchi, W. J. Youngblood, T. E. Mallouk, Y. Matsumoto, *J. Am. Chem. Soc.* **2008**, *130*, 7052–7059; b) M. A. Bizeto, A. L. Shiguihara, V. R. L. Constantino, *J. Mater. Chem.* **2009**, *19*, 2512–2525; c) M. Osada, T. Sasaki, *Adv. Mater.* **2012**, *24*, 210–228; d) S. Ida, Y. Okamoto, M. Matsuka, H. Hagiwara, T. Ishihara, *J. Am. Chem. Soc.* **2012**, *134*, 15773–15782.
- [6] a) B. P. Bastakoti, S. Guragain, Y. Yokoyama, S. Yusa, K. Nakashima, *New J. Chem.* **2012**, *36*, 125–129; b) S. O. Obare, N. R. Jana, C. J. Murphy, *Nano Lett.* **2001**, *1*, 601–603.
- [7] J. F. Gohy, N. Willet, S. K. Varshney, J. X. Zhang, R. Jérôme, *e-polymers* **2002**, 035.
- [8] a) N. Miyamoto, H. Yamamoto, R. Kaito, K. Kuroda, *Chem. Commun.* **2002**, 2378–2379; b) N. Miyamoto, T. Nakato, *J. Phys. Chem. B* **2004**, *108*, 6152–6159.
- [9] T. Sasaki, S. Nakano, S. Yamauchi, M. Watanabe, *Chem. Mater.* **1997**, *9*, 602–608.
- [10] a) Y. Kobayashi, H. Hata, M. Salama, T. E. Mallouk, *Nano Lett.* **2007**, *7*, 2142–2145; b) N. Miyamoto, K. Kuroda, *J. Colloid Interface Sci.* **2007**, *313*, 369–373; c) K. Maeda, M. Eguchi, S. H. A. Lee, W. J. Youngblood, H. Hata, T. E. Mallouk, *J. Phys. Chem. C* **2009**, *113*, 7962–7969.

Received: November 12, 2014

Published online: March 3, 2015